Towards Accurate Tumour Tracking in Lungs

Vincent Baudet, Pierre-Frédéric Villard, Fabrice Jaillet, Michaël Beuve, Behzad Shariat

Towards Accurate Tumour Tracking in Lungs.

Vincent Baudet, Pierre-Frédéric Villard, Fabrice Jaillet, Michael Beuve and Behzad Shariat
{vbaudet, pvillard}@liris.univ-lyon1.fr
LIRIS, bat Nautibus, 8 bd Niels Bohr, 69622 Villeurbanne CEDEX, FRANCE

Abstract

Motivated by radiotherapy and hadrontherapy improvement, we consider in a first step the potential of a simple elastic mechanical modelling to simulate lung deformations and motions during respiration, towards tumour tracking.

Two approaches are presented: one is the finite-element based method and the other is the mass-spring system. For these approaches, we suggest a personalisation based on the measurement of physical and geometrical data for each patient.

keywords : *conformal radiotherapy, hadrontherapy, lung compliance, finite elements, mass-spring systems, Young modulus*

1 Introduction

Conformal radiotherapy and hadrontherapy consist in delivering a lethal dose of ionising beam to the cancerous area, while reducing the impact on surrounding healthy tissues. Oncologists use safety margins around tumour to anticipate organ deformation and displacements. A current challenge is to reduce these magins and to produce a sophisticated method for these vulnerable organs.

To quantify the deformation and displacements of pulmonary tumours, the intensity and locality of the beam should be carefully evalueted so that the healthy tissues are unaffected.

This preliminary work presents a simulation of lung behaviour using two 3D dynamic deformable models to construct a model for the tumour displacement. A keypoint is that these models can be customised according to the patient's anatomy evaluated from CT scans and also from physiological paramaters such as the patient's compliance and breathing volumes.

This complex task was carried out systematically by initially focusing on simple elastic simulation of respiration and later producing the results to validate this approach.

2 Existing Models

Various approaches have been explored in modelling the surface of lung in three dimensional view. The models are catered mainly for information visualisation. Despite the fact that these models are made in depth purely for the surface (empty) representation, it is difficult or inappropriate to quantify any realistic tumour displacement or its internal mass or structure.

Among the other models, some global models study macroscopic structure behaviours and interactions while microscopic models focus on the alveolar structures and the air flow repartition.

Among the global models, two of the most realistic studies have been made by Kaye and Promayon. They are based on models incorporating medical specification such as anatomical and physiological but not personalised.

The model to which they mainly refer to is the one developped by Fung [12]. Fung described mechanical characteristics of the lung tissues by using a strain/stress law and obtained graphical representation based on experiments.

Promayon [10] developed a model that simulates trunk deformations under breathing. The model is based on physiological studies and defines precisely the different anatomical structures to be modelled. It also describes the geometrical relationship between each of them and their interactions. The model is focused on the diaphragm. Nevertheless, Promayon did not propose any solution for a personalised modelling of the patient's lung and other neighbouring organs.

Kaye [6] studied the kinematics of lung using mechanical approach, assuming a uniform external pressure and the lung with an elastic behaviour. In Promayon's model, the model well describes the interactions between the different anatomical structures in

the patient.

Amrani [1] developed a model based on particle systems deformed according to obstacles such as rib cage. However, the determination of the personalised parameters are found proceeding by trial and error.

Gefen [4] studied alveolar walls under electronic microscopy. The global mechanical characteristics are found thanks to the lung strain and are applied in a microscopic way to the alveolar walls. This model is restricted to dimension 2.

We did not focus on the microscopic models because of the insufficient medical data. Moreover, our aim is to provide a model as simple as possible.

Finaly the existing elastic models do not use personalised parameters or are not accurate enough to properly track tumours because of too many approximations.

3 Medical context and methods

Let us now introduce some notions about lungs and surrounding organs to better understand their influence on the tumour position during the treatment. Lungs are wrapped in a thin skin: the plevra. They are deformed under the diaphragmatic and rib-cage-muscle actions, which cause pressure changes inside the plevra, and consequently make lungs inflate or deflate. Due to their location, lung tumours could be very mobile (heart beating, diaphragm and thorax displacement) [7].

Our work is accomplished through a medical study in collaboration with the Léon Bérard cancer treatment Centre (CLB) and the respiratory physiology laboratory of the Louis Pradel hospital, both in Lyon, France. It is also related to an INRETS[1] anatomical study on lung and thorax mechanics.

Research protocols under investigation by our medical partners provide us with a wide range of informations. Profusion of data is necessary for preliminary studies, but, we must keep in mind that the final goal is to require a subset representing the most relevant data on patients' geometrical and associated physical parameters.

For this, an experimental protocol has been defined by oncologists, which provides us with thoracic CT scan examinations. The latters are grey level images representing the density in different slices. The CT-scan examination can be long (15 min) and during this process, organs can move and can provide rough data. To reduce the uncertainties in the tumours locations, we take the CT scan examination on a same patient at different periods of the respiratory cycle, measuring at each time the input air volume quantified with the help of an ABC system (Active Breath Control) [13]. This system is composed by a ventilator managed by a micro computer which controls the expiratory and inspiratory flows.

[1] Institut National de Recherche Sur les Transports et leur Sécurité

Air illustration of respiratory cycle is reproduced on (Fig.1).

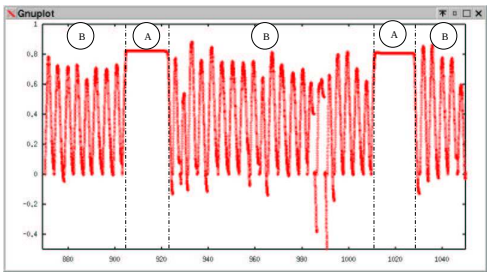

Figure 1. Air volume variation versus time (the breathing is blocked in A in order to obtain non blurred CT scan; the breathing is spontaneous in B)

It is possible to determine a position on the respiratory cycle and to block the breathing on this position. We obtain CT scans in blocked positions, therefore without any artifact, and for several lung positioning steps.

In the present study, four CT scans of thorax are processed. One is obtained during the spontaneous breathing and three others at different volume levels: one at the vital capacity volume and the two others above and below this volume. The latters will be very interesting for a clinical validation stage.

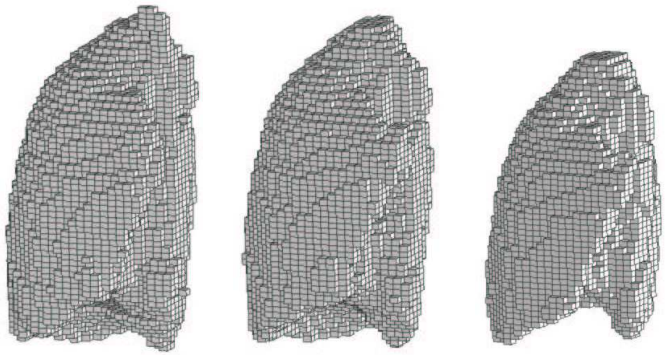

Volume:$3842cm^3$ Volume:$3621cm^3$ Volume:2380

Figure 2. Three states of the right lung during respiration

The three mesh plots in the Fig.2 show that there are differences between first and second plots taken respectively from inflating and deflating in spontaneous breathing. The last one shows the lung in maximum deflation, with the diaphragm well relaxed.

To model these shapes, we use segmentations of the CT scan for the right and left lungs, tumour and surrounding organs (Fig. 3). Finally, the mesh is constructed from these data.

Respiratory physiologic analysis realised at Louis Pradel hospital provides us with the compliance (C) [8], which represents the ratio of air volume varia-

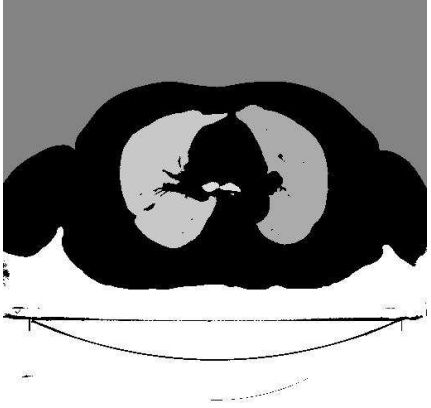

Figure 3. Segmented lungs image example

tion to the related air pressure variation. Lung compliance has two components: the first component is elastic and the second is surface tension. From the bulk modulus (K) definition [5], we associate the elasticity component to Young's modulus (E), the Poisson's ratio (μ) and the initial volume (V_i) according to eq. (1). E represents the coefficient relating stress and strain in the linear elasticity regim and μ is the measurement of the simultaneous change in elongation and in cross-sectional area within the elastic range during a tensile or compressive test.

$$K = \frac{E}{3(1-2\mu)} = \frac{V_i}{C} \tag{1}$$

Moreover, we consider thorax motion capture in this application. The separate functions of the diaphragm and the rib-cage influences may be revealed by a chest band or video sensors.

4 Suggested Models

We need a 3D model, which permits to process the particular tumoral behaviour of each patient. We have then to link the information previously described (§3) to a 3D deformable model. This approach is quite new since it combines both accuracy and personalisation.

We developped two models: the first one has proved its reliability in mechanics. It is a continuous media mechanics model resolved by the finite element technique. The second aims at optimising the computing time, which is one of the drawbacks of the first method. The latter is referenced to as hybrid method. For each method, we introduced mechanical laws based on physiological studies, and in particularly the compliance. The models monitoring is controled by a real breathing scenario obtained from patient's ABC recording.

4.1 Finite Element Method

This approach uses the physical laws from the continuous media mechanics formalisation (conservation laws, continuity, etc.). Beyond them are the constitutive relations that determine the peculiarities of a specific material. Various numerical techniques exist to solve this set of equations. We use the finite element technique.

The mechanical laws are driven by various kinds of equations and the variables are the displacement U and the stress σ.

The first equation is the balance equations in dynamics:

$$div\sigma + \rho.f = \rho.\ddot{U} \tag{2}$$

with f the bulk force density, ρ the volumic mass and $\ddot{U}$ the acceleration.

The kinematics equations link the strain ϵ to U and is expressed according to the Simo-Miehe law [11], which allows a great deformation state.

Then, the constitutive equation gives a relationship between ϵ and σ. We assume it to be:

$$\sigma = D.\epsilon \tag{3}$$

with D a 6×6 tensor, built with an homogeneous Young's modulus, and in an isotropic case defined by:

$$[D] = \frac{E}{(1+\mu)(1-2\mu)} \begin{bmatrix} \boxed{M_1} & 0 \\ 0 & \boxed{M_2} \end{bmatrix} \tag{4}$$

With:

$$M_1 = \begin{bmatrix} 1-\mu & \mu & \mu \\ \mu & 1-\mu & \mu \\ \mu & \mu & 1-\mu \end{bmatrix} \tag{5}$$

and

$$M_2 = \frac{1-2\mu}{2}[I_3] \tag{6}$$

$[I_3]$ is the 3×3 identity matrix.

Finaly, to resolve the problem, one has to state the boundary equations, which may be classified in two kinds and where a given set of data is symbolised by a g exponent:

- The surface constraint equations:

$$T = \sigma.n = T^g \tag{7}$$

  with T the surface constraint, n the exterior normal vector .

- The imposed displacements:

$$U = U^g \tag{8}$$

Lung geometry is modelled with a first CT scan mesh to obtain the initial state. It is an hexahedral mesh where each hexahedron is built up with eight points for each voxel. Besides, in a preliminary test, we have considered a lower resolution model, taking

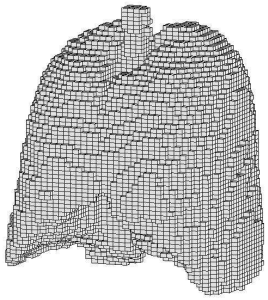

Figure 4. Lungs meshing example

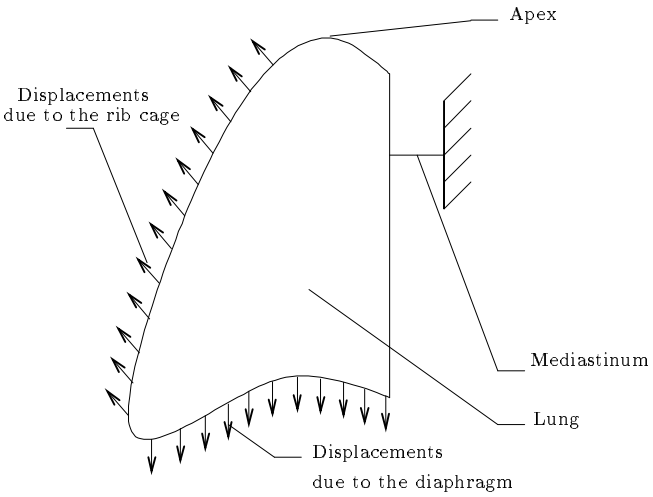

Figure 5. displacements scheme

only a 16 times less points per slice. From this clustering, we obtain $15 \times 15 \times 5$ mm hexahedrons. Fig.4 shows a lungs-meshing example made up of 6988 vertices and 4527 hexahedrons.

We compute the boundary conditions by imposing surface displacements as contact surface. The boundaries of the lung motion are modelled with next CT scan meshing representing the next state. A uniform normal pressure around the rib cage and around the diaphragm areas is applied to simulate the pleural elastic recoil pressure. Adding contact condition constrains with that boundary allows us either to block the displacement or to simulate the slipping skins (two blocked position stages are computed by this way). We leave the other areas unblocked except near the mediastinum where we set a zero displacement. Fig.5 shows these constraints.

Then, we can compute the displacements and stresses inside the lung. We give the surface displacement conditions. On the other hand, for the material parametrisation, we use the previously studied Young's modulus and the Poisson's ratio for bulk lung tissue, estimated to be $\mu \simeq 0.33$ [9]. For the intermediate states, an interpolation, not necessarily linear, parameterised by the thorax displacements and air breath volumes will be considered.

In the same way, we can compute the density on each vertex, with the relation (9) derivated from the mass conservation law.

$$\frac{d\rho}{dt} + div(\rho.\frac{d\vec{u}}{dt}) = 0 \tag{9}$$

4.2 Hybrid Method

In parallel, we develop a simulator software that combines different structure models, such as mass spring systems and implicit surfaces.

Implicit surfaces are restricted to the modelling of surfaces subject to small deformations such as rib cage and have the advantage to handle quickly the contact between objects. An implicit surface can be defined with a skeleton, which can be composed of elements such as vertices, edges or surfaces. They act as potential sources. The surface can then be defined by an equipotential around the skeleton (Fig. 6).

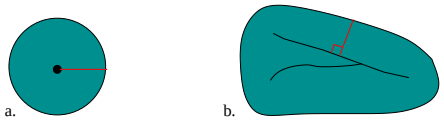

Figure 6. Skeleton implicit surface principle: a vertex skeleton with a constant potential value generates a sphere (a.), a more complex shape can be generated by incrementation of constant potential from some edges skeleton (b.)

Mass-spring systems are based on a volume mesh and are suitable to model general volumic behaviours.

We base our choice on Promayon and Amrani's studies [10, 1]. For lungs, we will use a tetrahedral mesh obtained from the segmented images (fig.3). Such a mesh is interesting to preserve the internal connectivity during deformations. For this, between each couple of nodes linked by a mesh edge, we apply a force of cohesion to keep the cohesion within the whole object.

A commonly used force is the linear elasticity given in eq.(10), with l_0 the distance between the two nodes at rest; l the new distance due to elongations generated by some constraints; and K the stiffness constant.

$$F = K(l_0 - l) \tag{10}$$

This kind of force description is well adapted for perfect elastic behaviour. However, living tissues do not follow this exact theoretical behaviour. Thus, another cohesion law [2] that is issued from particle system description may be used. This force is derivated from a potential field ϕ, with an energy of cohesion ϵ. This is given in eq.(12).

$$\vec{F} = g\vec{r}ad(\phi(l)) \tag{11}$$

$$\phi(l) = \frac{}{m-n}\left(m\left(\frac{}{l}\right) - n\left(\frac{}{l}\right)\right) \quad (12)$$

This equation shows the particle force evolution between two particles according to their distance and expresses repulsion and attraction behaviour [2].

The parameters of this equations can be linked to a local Young's modulus [1].

In the future, we will locally apply laws with different parameters in order to simulate the heterogeneous organ elasticity as in tumour areas.

To improve the quality of the simulation, we have linked the model to the pressure estimated from the ABC volume data and the compliance seen previously.

To inflate the lung we use the same method as Kaye or Promayon. It consists in applying orthogonal forces on the surface (Fig.7).

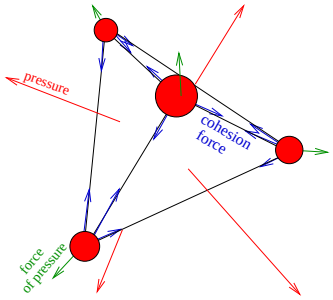

Figure 7. On each external triangle surface of the tetrahedral mesh, a pressure is applied, which generates forces of pressure at each external nodes and the consequently displacement implies the cohesion forces increase.

These forces are generated by pressure P on the surface as shown in equation 13, in which S_i represents a part of the surface. With this pressure, assuming homogeneity on the whole surface of the lung [8], we find the forces (F_i) on each vertex (of different tetrahedra) belonging to the surface of the organ.

$$\vec{F_i} = P\vec{S_i} \quad (13)$$

The pressure homogeneity is an approximation due to the global measurement of the compliance. We expect to correct it by combining both cohesion and inflating behaviours within the environmental constraints due to other anatomic structures such as rib cage, heart or diaphragm.

5 Results and Discussion

Fig.8 shows a simple illustration for the finite element nethod, computed with an open free software [3]. We apply perpendicular displacements around the rib cage and around the diaphragm and impose a zero displacement nearby the mediastinum. All the vertex displacements for the right lung were computed and represented in the figure by arrows of different length. The test were realised on a Pentium 4, 2.40GH with 1GB memory, the computing time was 3'44".

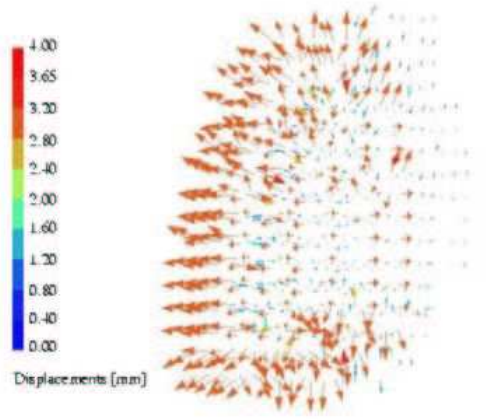

Figure 8. vertex displacements inside the lung represented by arrows

We note that the displacements are consistent with reality. Finally it is a first step to check if this numerical method can converge to plausible results. The next step, which consists in using a real displacement of external surfaces, is still under investigations.

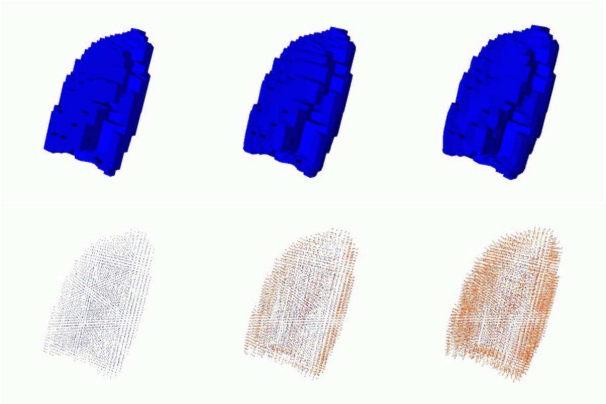

Figure 9. Lung state (at top) and displacements related to node mesh (at bottom) during ination according a sinusoidal breathing curve.

Fig. 9 shows a simple example of the hybrid method application. A meshed lung is inflated and deflated according a sinusoidal breathed volume. In this example, the lung volume well follows the imposed volume variation. The bottom images show the displacements from the rest position, on each node of the mesh. As no environmental constraints were applied, this displacements do not have any meaning. However, this illustrates our idea to be able to have an estimation of every displacement in the lung and in the future, in tumours.

6 Conclusion

In this paper, we presented two models to simulate lung inflation: continuous media mechanics model resolved by the finite element technique and spring mass system. Both models are developed in parallel and their results will be compared in order to build a more efficient model, taking into account both advantages. This work is the first step to solve the general problem of tumour tracking in lungs. The originality of the approach is the association of both accuracy and personalisation of the model to patients. The work is realised in a medical collaboration, which provide patient informations such as compliance and CT scan.

7 Future Work

Fisrtly, we may enhance the simulation by extending the environment (thorax, diaphragm, rib cage, etc.). This may allow to model contact contraints, heart beatings, tumours linked to other organs, etc.

To check the accuracy of our models, a study based on the pixels displacement analysis of images CT scan is in hand.

To the homogenety approximation, we may study a Young's modulus varying with the position. This may be avalable from the density information, provided by the CT scan.

We may also find out a more realistic lung behaviour including other phenomena such as viscosity and surface tension. We know that lung motions follow a hysterisis cycle and those kind of parameters may be helpful to reach this goal.

8 Aknowledgements

We thank all our partners: the Leon Bérard Centre, the ETOILE[2] project and the Ligue Nationale Contre le Cancer (the French League Against Cancer) for their support.

References

[1] Morade Amrani. *Modelling and simulating deformable objects*. PhD thesis, Université Claude Bernard Lyon, 2002.

[2] Morade Amrani and Behzad Shariat. Deformable organs modelling with multi layer particle system. *Information Visualisation 2000*, pages 351–356, 2000.

[3] Code Aster. http://www.code-aster.org/.

[4] A. Gefen and al. Analysis of stress distribution in the alveolar septa of normal and simulated emphysematic lung. *J. of Biomechanics*, (32), april 1999.

[5] C. Gerthsen and H. Vogel. *Physik*, volume 17. Springer-Lehrbuch, 1993. pp 118-119 § 3.4.1.

[6] J. Kaye, D.N.Metaxas, and F.P.Primiano. A 3d virtual environment for modeling mechanical cardiopulmonary interactions. *National Library of Medicine and the Philadelphia VAMC*, 1(LM-4-3515), 1998.

[7] K. M. Langen and D. T. L. Jones. Organ motion and its management. *Int. J. Radiation Oncology Biol. Phys.*, 50(1):265–278, 2001.

[8] Marylin L. Moy and Stephen H. Loring. Compliance. *Seminar in respiratory and critical care medecine*, 19(4):349–359, 1998.

[9] M.R. Owen and M.A. Lewis. The mechanics of lung tissue under high-frequency ventilation. *SIAM Journal on Applied Mathematics*, 61(5):1731–1761, 2001.

[10] E. Promayon. *Modelling and simulation of the respiration*. PhD thesis, Université Joseph Fourier de Grenoble, 1997.

[11] J.C. Simo and C. Miehe. Associative coupled thermoplasticity at finite strains: formulation, numerical analysis and implementation. *Comp. Meth. Appl. Mech. Eng.*, 98:41–104, 1992.

[12] D.L. Vawter, Y.C. Fung, and J.B. West. Constituve equation of lung elasticity. *Journal of Biomechanical Engineering*, (101):38–45, 1979.

[13] J. W. Wong and al. The use of active breathing control (abc) to reduce margin for breathing motion. *Int. J. Radiation Oncology Biol. Phys.*, 44(4):911–919, 1999.

[2] E.T.O.I.L.E.: Espace de Traitement Oncologique par Ions Légers, http://ETOILE.univ-lyon1.fr